International Congress Series 1265 (2004) 275–280

www.ics-elsevier.com

Assessment of the precision in co-registration of structural MR images and PET images with localized binding

Peter Willendrup, Lars H. Pinborg, Steen G. Hasselbalch, Karen H. Adams, Karin Stahr, Gitte M. Knudsen, Claus Svarer*

Neurobiology Research Unit, Rigshospitalet, Blegdamsvej 9, N9201 Copenhagen 2100, Denmark

Abstract. The aim of the present study was to access and compare the accuracy and reproducibility of two fully automatic and two manual methods for co-registration of structural T1-weighted MR images and functional images with localized binding. It is concluded that for functional images with distributed binding all over the brain, such as F18-FDG images, the automatic methods are preferable, while for images with localized binding, such as F18-Altanserin 5-HT_{2A} neuroreceptor images, it is essential to use methods that handle this special problem, like the proposed manual methods.

Keywords: Co-registration; Alignment; MR; PET; Neuroreceptor images

1. Introduction

In functional brain images with only localized tracer binding, e.g. some receptor PET images, the lack of sufficient structural information prevents a correct identification of relevant brain structures. In this case, a correct co-registration of the functional image to a structural brain image, e.g. MR, is difficult. In this context, co-registration is the process of spatial reorientation of one of the images to match the other image, thereby identifying the translation and rotation parameters.

A variety of automatic and manual methods are available for co-registration of functional and structural images. The manual methods are based on visual inspection, corrections where one or both of the images are translated and rotated to match the other, with these steps repeated until a satisfying match is obtained. With the semi-automatic method, the observer identifies corresponding points in both images and the images are then automatically co-registered. Automatic methods are either based on surface matching or minimization of a cost-function defined by matching voxels [1,4,12] from each of the image modalities.

* Corresponding author. Tel.: +45-3545-6716; fax: +45-3545-6713.
E-mail address: csvarer@nru.dk (C. Svarer).

0531-5131/
doi:10.1016/j.ics.2004.04.065

As described previously by West et al. [11] and Pfluger et al. [8], the automatic methods are sufficient for most functional PET images and are preferable because they are less time-consuming, more objective and have a slightly higher precision. In contrast, for PET images with localized binding, the automatic methods are likely to have serious shortcomings.

The aim of this study is to determine the effectiveness of four different methods for co-registration of F18-Altanserin 5-HT_{2A} neuroreceptor images and T1-weighted MR images. Since the cerebellum is almost void of 5-HT_{2A} receptors, the PET images are difficult to co-register with MR images, at least by means of automatic methods.

2. Methods

Four co-registration methods were tested:

- Interactive Point Selection, IPS (semi-automatic method implemented at NRU).
- Interactive Image Overlay, IIO (manual method implemented at NRU).
- Automatic Image Registration, Air 5.0 [12].
- Statistical Parametric Mapping, SPM 99 [1].

In total, five sets of corresponding, simulated F-18 FDG PET images, F-18 Altanserin receptor PET images, and T1 MR images were co-registered using all four methods.

A panel of seven users tested the two manual methods implemented at NRU to assess the inter- and intra-user variability and reproducibility of each method. Four times, once a week, they performed manual alignment of each of the five data sets by means of both of the manual methods.

The two automatic methods were applied to MR images where the skull has been removed using the BET[1] software [9]. Standard parameter settings were used.

The simulated PET images were created to emulate F-18 FDG images, as illustrated in Fig. 1. After removal of the skull the MR image was segmented into background, gray and white matter and reasonable values were assigned to each tissue type (BG-0, WM-1 and GM-4). Also, the skull segment was re-added, scaled to a maximum value of 0.5. Then the image was filtered with a Gaussian filter ($6 \times 6 \times 8$ mm) and down-sampled from MR to PET resolution ($2 \times 2 \times 4.25$ mm), Radon transformed, random noise was added, and images were reconstructed using a filtered back-projection algorithm. The images were randomly reoriented (uniform distribution) before creating the Radon projections, with maximum translation parameters of 2 cm in each axis direction and rotated maximally 10° around each image axis.

2.1. Interactive point selection (IPS)

This method is based on the observer pointing out several identical landmarks (x_j. and x_j') in both modalities. Ideally, only three corresponding points are required, but to minimize the error, a total of six points were demanded. From the point definitions, a homogenous transformation matrix A ($x_j' = A \cdot x_j$) is calculated by minimization of the cost-

[1] Software homepage http://www.fmrib.ox.ac.uk/analysis/research/bet/.

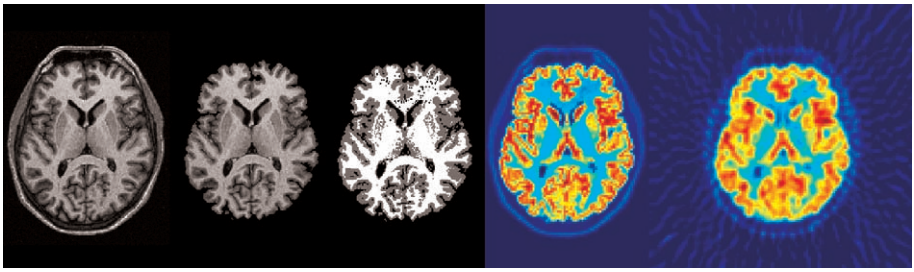

Fig. 1. Visualization of the generation of a simulated PET image (see text for details). (A) The original MR image. (B) MRI without skull. (C) Segmented MRI into background, gray and white matter. (D) Standard FDG PET values (GM/WM ratio=4) have been assigned and the image has been filtered. (E) Simulated "F-18 FDG image".

function $E(A(t,\phi)) = \Sigma_j (A(t,\phi)x_j - x_j')^2$ with respect to the three-dimensional translation and rotation parameters t and ϕ [5]. After calculation of A, the user is presented with an error measure $e(x_j, x_j', A(t,\phi)) = |x_j A(t,\phi) - x_j'|$ for each of the defined landmark points (x_j, x_j'). This can then be used for evaluation of the precision of each point pair and, in case of unacceptable error values, the relevant steps can be repeated.

2.2. Interactive image overlay

This method is inspired by Pfluger et al. [8], but modified to include both contours and overlays. Initial registration is done by registering the center of mass of the two images, and afterwards the user interactively rotates or translates three transparent slices and contours from the PET image displayed on top of the MR. This step is repeated until the user is content with the result, and a six-parameter transformation matrix A is calculated.

For the simulated PET images, the perfect co-registration parameters B $(x_j' = B \cdot x_j)$ between PET and MR images are known. These parameters were used as the gold standard for testing the performance of the different methods. For the Altanserin PET images, however, the true co-registration parameters were estimated from the mean alignment parameters resulting from all the manual alignments ($n = 56$). This approach for generation of "true" transformation parameters B was tested at the simulated PET images. The way to calculate the performance is to randomly sample 10,000 voxel coordinates inside the brain mask generated using the segmentation from BET software. The coordinates were then forward-projected using the estimated transformation parameters and backward-projected using the inverse of the "true" transformation as described in the equation $x_j'' = B^{-1} \cdot A \cdot x_j$. Calculating the mean distance $E_{\text{cost}} = \Sigma_j (x_j - x_j'')^2$ between the original coordinates and the forward–backward transformed coordinates then gives the mean precision of the methods, evaluated over all brain voxels. This evaluation is similar to the region-based method presented in Refs. [3,7,11].

3. Results

Fig. 2 (left panel) shows that with both of the manual methods, a precision of approx. 3.6 mm was achieved for the simulated PET data, in accordance with results reported in the literature as in West et al. [11]. The two automatic methods generated a precision of

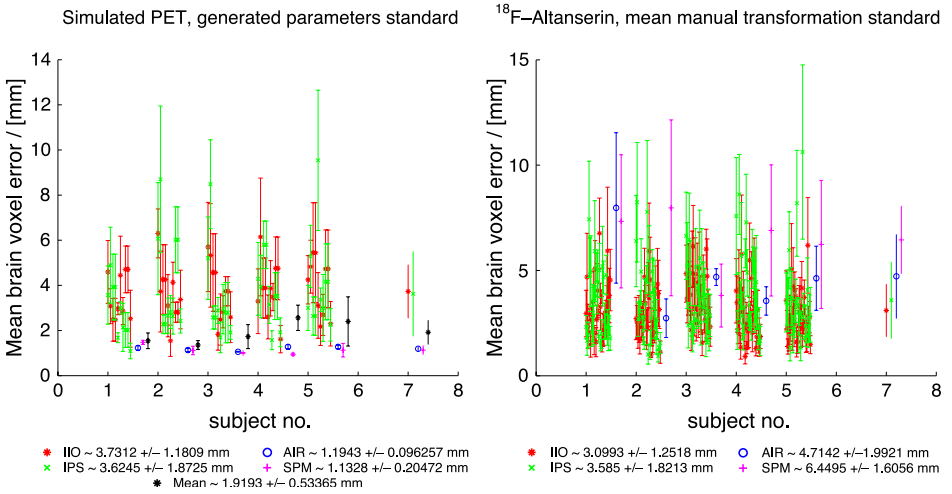

Fig. 2. Results of co-registration using the different approaches. Left panel: simulated FDG PET image. Right panel: real F-18 Altanserin PET image.

approx. 1.15 mm, which is somewhat better than reported in the literature for real (non-simulated) image sets. This finding was not unexpected, due to the way that the PET data were generated, directly from the MR images. Using the mean of the manual transformations as the gold standard was also tested. The precision of the average manual transformation was about 1.9 mm, indicating that with an accuracy of about 1.9 mm, the mean manual transformation can be used as a gold standard transformation, when no known true transformation is available.

Fig. 2 (right panel) shows that using the mean manual transformation as gold standard for co-registration of ^{18}F-Altanserin images, the two automatic methods, SPM and AIR, performed less well than either of the manual methods, and this was also supported by visual inspection, cf. Fig. 3. Particularly for cerebellum, the automatic approaches tend to mis-registrate, trying to incorporate other brain regions into the cerebellum. The order of the found misalignment errors are in good agreement with the results reported in the literature [2,6,10].

In Table 1, the time consumption to arrive at the final result is reported for both manual methods. The Interactive Image Overlay method took about half as long as the Interactive Point Selection method ($p < 0.05$). It is seen that these users, unfamiliar to either methods, improved their performance after the first trial week.

4. Discussion

For the simulated images, SPM and AIR were clearly superior to the manual methods, indicating that for functional images where tracer binding is evenly distributed to all gray or white matter brain voxels the automatic methods are preferable. Although the precision was not significantly better than for the manual methods, the automatic methods are more objective and time-saving.

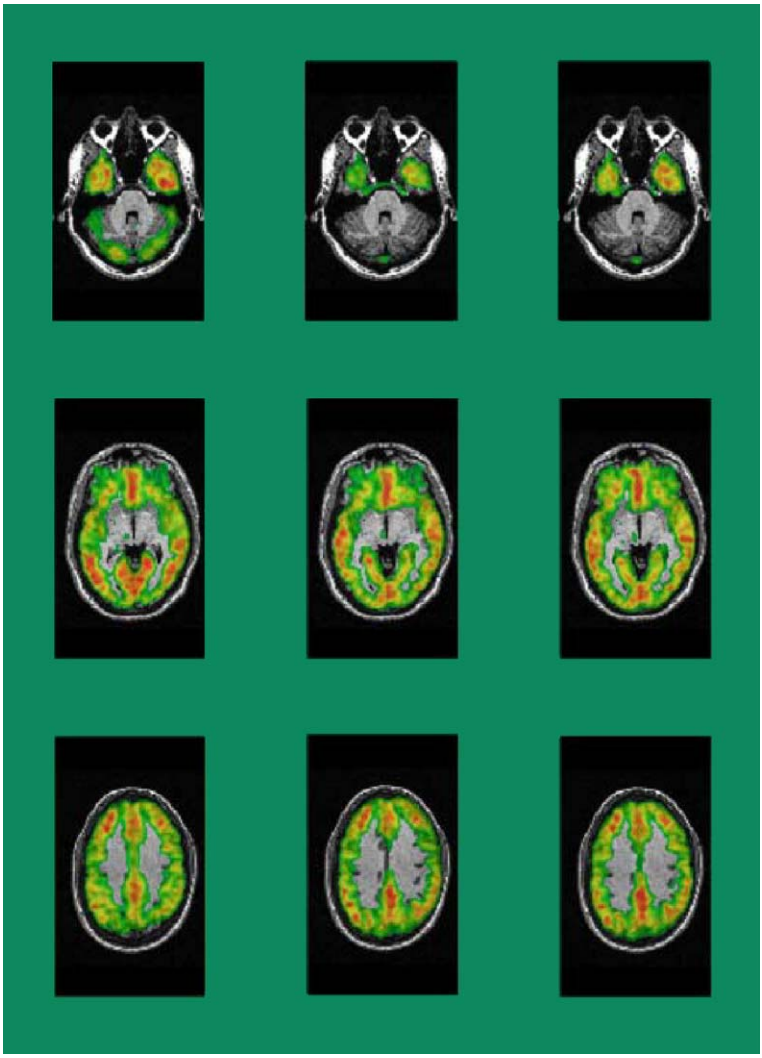

Fig. 3. Visual inspection of co-registrations. Left panel: SPM, middle panel: AIR, right panel: average result of both manual methods.

Further, we demonstrate that in the absence of gold standard parameters, the mean registration of the manual methods can be used. It has previously been shown that external, fiducial markers can be used for identification of the co-registration parameters [3,11], but this requires that the scannings are conducted at least on the same day, which is not applicable at most sites.

For the Altanserin images, the manual methods yielded a lower error than the automatic methods did, with errors being comparable with those reported in the literature. It is concluded that for functional images where the tracer is (almost) equally distributed over

Table 1
Average ± standard deviation time consumption in minutes for both methods over trial weeks

Methods	Week 1	Week 2	Week 3	Week 4	All weeks
IIO	13.4 ± 5.9	9.4 ± 3.6	9.5 ± 2.5	8.9 ± 3.5	10.3 ± 4.5
IPS	27.4 ± 7.5	20.1 ± 4.9	21.0 ± 3.8	17.3 ± 4.4	21.5 ± 6.6

the brain, the automatic methods are preferable, while for images with localized tracer binding, manual methods are superior. Alternatively, template images specifically designed for tracers with confined binding could be constructed and tested together with the automatic methods.

Acknowledgements

The EU fifth framework program QLG3-CT2000-00594 PVEOut is thanked for funding the project.

References

[1] J. Ashburner, K. Friston, Multimodal image coregistration and partitioning—a unified framework, NeuroImage 6 (1997 Oct.) 209–217.
[2] L.G. Brown, A survey of image registration techniques, ACM Comput. Surv. 24 (1992 Dec.) 325–376.
[3] J.M. Fitzpatrick, J.B. West, C.R. Maurer Jr., Predicting error in rigid-body point-based registration, IEEE Trans. Med. Imag. 17 (1998 Oct.) 694–702.
[4] S.J. Kiebel, et al., MRI and PET coregistration—a cross validation of statistical parametric mapping and automated image registration, NeuroImage 5 (4 Pt. 1) (1997 May) 271–279(1053-8119).
[5] G.Q. Maguire Jr., et al., Graphics applied to medical image registration, IEEE Comput. Graph. Appl. 11 (1991) 20–28.
[6] J.B. Maintz, M.A. Viergever, A survey of medical image registration, Med. Image Anal. 2 (1998 Mar.) 1–36.
[7] C.R. Maurer Jr., et al., Registration of head volume images using implantable fiducial markers, IEEE Trans. Med. Imag. 16 (1997 Aug.) 447–462.
[8] T. Pfluger, et al., Quantitative comparison of automatic and interactive methods for MRI-SPECT image registration of the brain based on 3-dimensional calculation of error, J. Nucl. Med. 41 (2000 Nov.) 1823–1829.
[9] S.M. Smith, Fast robust automated brain extraction, Hum. Brain Mapp. 17 (2002 Nov.) 143–155.
[10] S.C. Strother, et al., Quantitative comparisons of image registration techniques based on high-resolution MRI of the brain, J. Comput. Assist. Tomogr. 18 (1994 Nov.–Dec. 31) 954–962.
[11] J. West, et al., Comparison and evaluation of retrospective intermodality brain image registration techniques, J. Comput. Assist. Tomogr. 21 (1997 Jul.–Aug. 31) 554–566.
[12] R.P. Woods, J.C. Mazziotta, S.R. Cherry, MRI-PET registration with automated algorithm, J. Comput. Assist. Tomogr. 17 (4) (1993 Jul.–Aug. 31) 536–546 (0363-8715).